Catalysis Science & Technology

Accepted Manuscript

ROYAL SOCIETY OF CHEMISTRY

www.rsc.org/catalysis

Oleic acid decarboxylation over Pt- supported on small pore zeolites and hydrotalcite catalysts

M. Ahmadi [a], A. Nambo [a], J.B. Jasinski [b], P. Ratnasamy[b,c] , M.A. Carreon[* d]

Keywords: decarboxylation, isomerization, fuel hydrocarbons, zeolites, hydrotalcite

Abstract

The catalytic decarboxylation and further conversions of oleic acid to paraffins, branched and aromatic hydrocarbons over Pt supported on small pore zeolites and hydrotalcite is demonstrated. The influence of support, platinum source, and reaction temperature on the decarboxylation of oleic acid were investigated. An increase of reaction temperature increased the degree of decarboxylation and selectivity to heptadecane. Pt-SAPO-34 was a very effective catalyst. In addition to a high degree of decarboxylation, Pt-SAPO-34 displayed a high selectivity to heptadecane and dodecylbenzene among the products. Branched isomers, cracked (mostly < C17) paraffins, alkenes such undecene, dodecene and carboxylic acids such nonanoic acid, decanoic acid were observed as side products. The further isomerization of the initially formed linear heptadecane (by decarboxylation of oleic acid) to branched isomers is suppressed in the narrow pores of SAPO-34 due to restricted transition state shape selectivity limitations in the pore system of SAPO-34. Catalyst acidity, dispersion of Pt and pore diameter of the support played crucial roles in determining product selectivity.

1. Introduction

Biofuel production technologies have recently received considerable attention as CO_2 emission of biofuels is lower compared to conventional fuels[1]. Some of the sources of biofuels are natural oils and fats (e.g., animal fats, plant and seed oils). They are complex mixtures of triglycerides, which are fatty acid esters of glycerol. The carbon chain lengths of the fatty acids range from about C_8 to C_{24}, but C_{12}, C_{16}, and C_{18} fatty acids tend to be the most abundant [2].

Removing oxygen from fatty acids (deoxygenation) leads to the formation of paraffinic hydrocarbons that can potentially serve as or be converted to direct replacements for traditional petroleum-derived liquid transportation fuels and paraffinic petrochemical feedstocks [3].Deoxygenation of unsaturated fatty acids are accomplished via hydrogenation of double bonds and further removal of the carboxyl group by releasing carbon dioxide and producing a paraffinic hydrocarbon (decarboxylation) or by releasing carbon monoxide and producing an olefinic hydrocarbon (decarbonylation) [4-7]. Intensive studies on liquid phase deoxygenation of free fatty acids and fatty acid esters have been carried out [6-15]. Metals such as Ni, Ni/Mo, Ru, Pd, Pd/Pt, Pt, Ir, Os and Rh supported on different supports have been evaluated for their deoxygenation performance under elevated temperatures and pressures. The effect of the nature of the carrier gas on conversion and selectivity values were investigated by previous groups. Maier *et al.* [16] deoxygenated aliphatic and aromatic carboxylic acids over Pd/SiO_2 and Ni/Al_2O_3 catalysts at 330°C in different environments (H_2 or N_2) in the gas phase and found that the presence of hydrogen is desirable to maintain stable catalytic activity during the decarboxylation reaction. In contrast, no reaction occurred in a nitrogen atmosphere. Snare *et al.* [7] conducted liquid phase deoxygenation experiments in a continuous flow reactor under Ar and H_2 atmosphere and solvent-free conditions using a Pd/C catalyst. However, the formation of hydrocarbons, mainly olefins and aromatics, were below 10 mol%. Representative examples of catalysts employed for the conversion of stearic acid to heptadecane include selenium [17], complexes of Pd and Rh [18], and Pd-C [19]. However, in these studies, the yield to heptadecane or stearic acid conversion was low. Some studies of the decarboxylation of the unsaturated oleic acid have also been reported [7, 20-23]. In most of the above studies, the support has been catalytically inert material (like carbon) or relatively, non-acidic components, like silica or non-acidic alumina. To our best knowledge, the influence of stronger acidic supports in modifying the carbon skeleton of the linear C_{16}- C_{18} paraffins (initial products of the decarboxylation of the fatty acid), by isomerization, cracking, cyclization, hydrocracking *etc.,* has not been explored. By contrast, the hydrocracking and isomerization reactions of hydrocarbons, especially those boiling in the gasoline range (C5-C10), over Pt supported on strongly acidic supports (like Pt- Zeolites) has been extrensively studied. The strength and surface density of the acidic sites as well as the pore diameter of the acidic support are known to influence the hydrocarbon distribution among the products. To satisfy the application requirements of the diesel vehicles hydrocarbons with different conformation

(paraffin mixtures) should be produced from triglycerides and fatty acids. As these normal paraffin (mainly n-C_{12} to n-C_{-20}) mixtures have high cetane number, they have excellent performance. On the other hand, the pour point of these paraffin mixtures is high so their structure should be modified to fulfill the requirements of the diesel blending components (the pour point should be below 5°C). For this purpose the catalytic isomerization of the normal to isoparaffins is, often, used to lower their pour points [24, 25].

Hydroisomerization reactions of normal paraffins are carried out in the presence of the bi-functional catalysts. The degree of isomerization, the product yield and composition are significantly affected by the properties of the used catalyst (acidity, surface area and pore size distribution), the applied operational parameters (temperature and pressure). Isomerization takes place easily in the presence of different noble metal containing zeolites (ZSM-5, ZSM-22), mesoporous structures (MCM-41, Al-MCM-41) and silica-alumina-phosphates (SAPO-11, SAPO-31, SAPO-41) as they have mild acidity [25]. Some catalysts like SAPO-11, SAPO-31, SAPO-41 were found to be favorable for the isomerization of long chain paraffins [26]. Isomerization of paraffins over Pt-SAPO-11, Pd-SAPO-11, Pt-SAPO-5 were reported in the literature [25-29]. In addition to acidity, the pore diameter of the catalyst also plays a crucial role in determining product selectivity.

If the deoxygenation of the fatty acid and subsequent isomerization / hydrocracking of the resulting C_{17}- C_{18} linear paraffins to branched, gasoline-range C_5- C_{10} hydrocarbons with lower pour points and higher octane numbers can be accomplished by a bifunctional catalyst in a single reactor, it will represent a significant advance in the process of conversion of lipid biomass material to 'drop-in' hydrocarbon transport fuels, like motor and aviation gasoline. In our previous work we have demonstrated the catalytic decarboxylation and further conversion of oleic acid to branched and aromatic hydrocarbons in a single process step, over Pt–SAPO-11 and Pt/chloride Al_2O_3 [30]. Herein, we report the catalytic decarboxylation of oleic acid and further conversion of the resulting linear paraffins over catalysts of varyig acidity and pore diameter, Pt/SAPO-34, Pt/DNL-6, Pt/Rho and Pt/hydrotalcite, in a single process stage. Such an investigation has not been reported, so far.

2. Experimental

2.1 Catalyst preparation and characterization:

2.1.1 Synthesis of SAPO-34

SAPO-34 is a silicoaluminophosphate zeolite having composition $Si_xAl_yP_zO_2$, where x = 0.01-0.98, y = 0.01-0.60, and z = 0.01-0.52 with ~0.38 nm unimodal micropores [31]. In a typical synthesis, the Al source (99.9% $Al(i\text{-}C_3H_7O)_3$), H_3PO_4 and deionized water were stirred for 3 h to form a homogenous solution and then Ludox AS-40 colloidal silica (40 wt% suspension in water Sigma-Aldrich) was added and the resulting solution was stirred for 3 h. Tetraethyl ammonium hydroxide (TEAOH, 35 wt% solution in water Sigma-Aldrich), dipropylamine (99%, Aldrich) and cyclohexylamine (99% Sigma-Aldrich) were added and the solution was stirred for 4 days at 60°C. The solution was then transferred into a stainless-steel autoclave and held at 220 °C for 24 h. Then, the autoclave

was cooled down and the solid product was separated by centrifugation and washed three times with deionized water. Finally, SAPO-34 was dried and then calcined at 550°C for 5 h (the calcination heating and cooling rates were 1 and 2 °C/min, respectively).

2.1.2 Synthesis of DNL-6

DNL-6 is a silicoaluminophosphate molecular sieve with the RHO framework having pore size of ~0.36 nm [32]. The synthesis of DNL-6 was as follows: 1.17g orthophosphoric acid (85 wt%) and 0.625g tetraethyl orthosilicate were mixed with a solution of 3.06g aluminium isopropoxide and 13.5g deionized water, and then an aqueous solution of cetyltrimethylammonium bromide (CTAB) was added with final addition of 1.097g of diethylamine (DEA). Stirring was kept during all the above mixing procedure. The specific gel composition for the hydrothermal synthesis was: Al: P: Si: DEA: CTAB: H_2O= 1: 0.8: 0.2: 1: 0.1: 50. The final gel mixture was transferred into a stainless-steel autoclave and held at 200 °C for 24 h. After 24 h, the autoclave was cooled down and the solid product was collected by centrifuge, washed three times with deionized water and dried at 110°C overnight. Calcination was carried out at 600 °C for 4 h to remove organic species (the calcination heating and cooling rates to remove organic species were 1 and 2 °C/min, respectively).

2.1.3 Synthesis of RHO

RHO zeolite consists of a body centered cubic arrangement of LTA cages displaying an average pore size of ~0.36 nm [33, 34]. In a typical synthesis, 0.94 g of crown ether 18-C-6, 0.705 g of CsOH and 0.34 g of NaOH were dissolved in 6.04 g of distilled water. Then, 1.32 g of sodium aluminate was added to the above solution and the resulting mixture was stirred until a clear solution was formed. Subsequently, 10.5 g of colloidal silica (Ludox AS-40) were added and the resulting reaction mixture was stirred at room temperature for 24 hours. The final gel composition was: 1.8 Na_2O : 0.3 Cs_2O : Al_2O_3 : 10 SiO_2 : 0.5 R : 100 H_2O (where R is the crown ether 18-C-6).Zeolite crystallization was carried out in an autoclave at 150 ^oC for 1 day. The zeolite Rho recovered after filtration, washing with water and drying at 100 ^oC overnight. Then it was calcined at 500 ^oC for 3 hours to remove organic species (the calcination heating and cooling rates to remove organic species were 1 and 2 °C/min, respectively).

2.1.4 Synthesis of Hydrotalcite

A basic Zn-Al based hydrotalcite with expected interplanar spacing of 0.75 nm was prepared. Hydrotalcite was synthesized using the conventional precipitation method [35]. In a typical synthesis, 200 ml solution containing 0.126 M $Zn(NO_3)_2$ and 0.063M $Al(NO_3)_3$ was prepared. The solution was stirred and heated at 85°C, then a stoichiometric amount of urea was added and the solutions was kept under reflux for 24 hours, then filtered and washed with boiling water several times.

The four supports were impregnated with two different sources of Pt (potasium hexachlorplatinate and tetraamine Pt nitrate, denoted as salt 1 and 2 respectively) at 5 %wt.

0.126 g of Pt source (salt 1 or salt 2) was dissolved in deionized water (0.7 cm^3/g-support) and then impregnated over the support meanwhile the suspension was stirred. The

mixture was further dried overnight at 100°C following by calcination at 400°C for 5 hr and then reduction in flowing hydrogen at 450°C for 2hr to remove the ligands of the precursor and to reduce the metal to its active elemental state. The Pt ions in the impregnating solution will have access to the pores of all the catalysts used in this study. Catalytic activity, however, is determined by the access of the reactant, oleic acid, to the Pt sites. In view of the large size of the oleic acid molecule (especially of the cis isomer, the predominant fraction) and the small pore diameter of SAPO 34, RHO and DNL-6, most of the decarboxylation reactions(for which the active sites are the Pt sites) are expected to occur on the outer, exposed surface of these molecular sieve catalysts.

The catalysts were characterized by X-ray diffraction (XRD), nitrogen adsorption (BET), transmission electron microscopy (TEM) and scanning electron microscope (SEM). XRD patterns were collected on a Bruker D8 Discover diffractometer at 40 kV and 40 mA with Cu Kα radiation. BET surface areas and N_2 adsorption-desorption isotherms were collected in a Micromeritics Tristar-3000 porosimeter at 77 K using liquid nitrogen as coolant. Before measurements, the catalyst was degassed at 150 °C for 3 h. Transmission electron microscopy (TEM) was used to inspect the morphology of catalysts. TEM images were taken on Technai F20 FEI TEM using a field emission gun, operating with an accelerating voltage of 200kV. The scanning electron microscopy (SEM) was performed on a FE-SEM (FEI Nova 600), with an acceleration voltage of 6 kV.

2.2 Reaction procedure:

Oleic acid (90%, Alfa-Aesar) was used as the unsaturated fatty acid. Before reaction, the catalysts were pre-activated in dry nitrogen in the oven for 3 hrs at 150°C. The degassing temperature (150°C) was chosen (from thermogravimetric studies of the catalyst) to ensure the removal of all adsorbed H_2O. 3 h was found to be adequate to remove all the adsorbed water. In the absence of the above preactivation, catalytic activity was low presumably due to the retarding effect of adsorbed H_2O molecules. The decarboxylation reactions were conducted in a 250 mL stainless steel, high pressure autoclave reactor (Parr model 4576A). Oleic acid and catalyst were loaded into the reactor with a mass ratio of 20:1. Before the reaction started, the reactor was flushed with H_2 and the pressure was increased to the desired reaction pressure (usually 20 bar). Under constant stirring conditions, the reactor was heated at a rate of 10°C/min to the reaction temperature (245 and 325°C). The catalysts were reduced in hydrogen at 200 °C and a pressure of 20 bar for 2 h. One mole of H2 is needed for conversion of oleic acid to heptadecane. The reaction conditions (temperature (200-350°C), H2 pressure and reaction time of 2 h) were chosen from our previous experience in the decarboxylation of fatty acids [30] to optimize the yield of hydrocarbons. At longer reaction times cracked products (< C9) were observed in significant quantities. After the reaction, the catalyst was separated, by filtration, from the liquid product and washed with acetone for further characterization.

2.3 Product analysis:

Besides the organic liquid and gas phase hydrocarbons, a small amount of water was also observed in some cases.

However, the amount was too small to be analyzed quantitatively. The liquid phase product withdrawn from the reactor was analyzed with a gas chromatograph (GC, 7820 A) equipped with a HP-5 MS column (with dimensions of 30 m × 250 µm × 0.25 µm) and a 5975 MSD detector. For the analysis, the samples were silylated with *N,O*-bis(trimethyl)-trifloroacetamide, BSTFA (Acros organics, 98%). After addition of silylation agent, the samples were kept at 60°C for 1 hr. Silylation was incomplete at lower temperatures and shorter times. A sample of 0.2 µL was injected into the GC column (225°C, 10.5 psi) with a split ratio 20:1, and the carrier gas (helium) flow rate was 1 mL/min.22. The following temperature program of the gas chromatograph was used for analysis: 100°C for 5 min, 300°C (20°C/min, for 2 min). Quantitative analysis was accomplished by generating and using calibration curves for each compound of interest. The product identification was confirmed with a gas chromatograph - mass spectrometer (GC-MS).

Acid number.

The decarboxylation conversion of the oleic acid was estimated from the reduction in the number of oleic acid carboxylic acid groups during the reaction. The amount of carboxylic acid groups remaining in the products after the reaction was evaluated by quantifying the acid number (ASTMD974). Acid number is the mass of potassium hydroxide (KOH) in milligrams that is required to neutralize one gram of chemical substance.

To quantify the acid number, a known amount of sample (about 0.1g) is dissolved in a solvent (ethanol + Petroleum ether), then titrated with a solution of sodium hydroxide (NaOH, 0.1N) using phenolphthalein as a color indicator.

The acid number is calculated from this equation:

$$Acid\ number = 56.1\frac{NV}{W}$$

N= 0.1 (N)

V= volume of NaOH consumed (ml)

W= mass of the sample (g)

The decarboxylation % was calculated using the acid number of oleic acid and acid number of the product using the following relation:

% Decarboxylation= (acid number of oleic acid- acid number of the product) / acid number of oleic acid × 100%

3. Results and Discussion

The SEM images of RHO, DNL-6 SAPO-34and hydrotalcite supports are shown in Figure 1. Figure 1a shows a representative SEM of RHO showing spherical morphology with average of ~1.5 µm. Figure 1b shows a representative SEM of DNL-6 showing hexagonal-like morphology with average size of ~2.5 µm. Figure 1c shows a representative SEM of SAPO-34 showing cubic like morphology with average size of 2.3 µm Figure 1d shows a representative SEM of hydrotalcite showing irregular ~3 µm agglomerates composed of needle-like shapes.

Figure 2 shows the XRD patterns of all studied Pt-supported catalysts. Figures 2a and 2b show the XRD patterns of Pt-RHO and Pt-DNL-6 respectively. Both are in agreement with the RHO topology [34]. .Figure 2c shows the XRD pattern of chabazite structure, typical topology of SAPO-34 [36]. Figure 2d shows the typical layered

structure of the Mg-Al based hydrotalcite corresponding to an interplanar spacing of ~ 0.7 nm

The BET specific surface area of the supports and Pt/supports are given in Table 1. As expected, in all cases, the surface area decreased with the incorporation of Pt. Interestingly, when salt 2 was used as Pt source the decrease in surface area was less pronounced, suggesting a better dispersion of Pt when salt 2 was employed**.** N_2 BET measurements on zeolite Rho were unsuccessful (no measurable N_2 adsorption was observed). This is not uncommon, since the effective pore aperture of dehydrated zeolite Rho is ~2.9 Å [33] making difficult for N_2 (kinetic diameter ~3.6 Å) to adsorb within the zeolite pores.

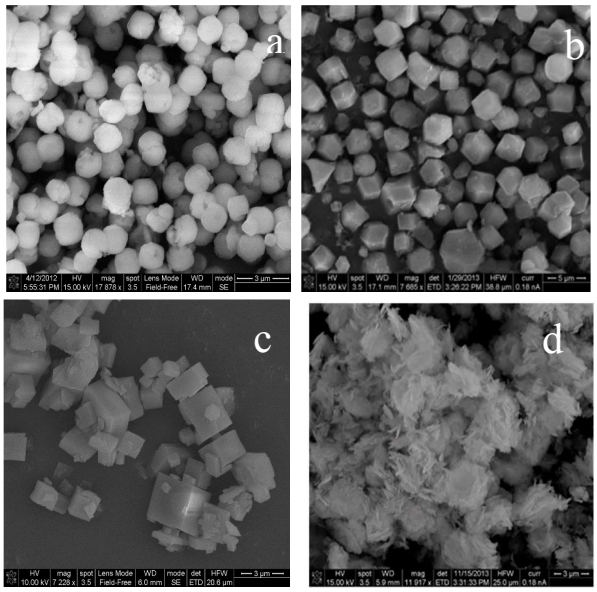

Figure 1. SEM images of a) RHO, b) DNL-6 and c) SAPO-34 d) Hydrotalcite supports

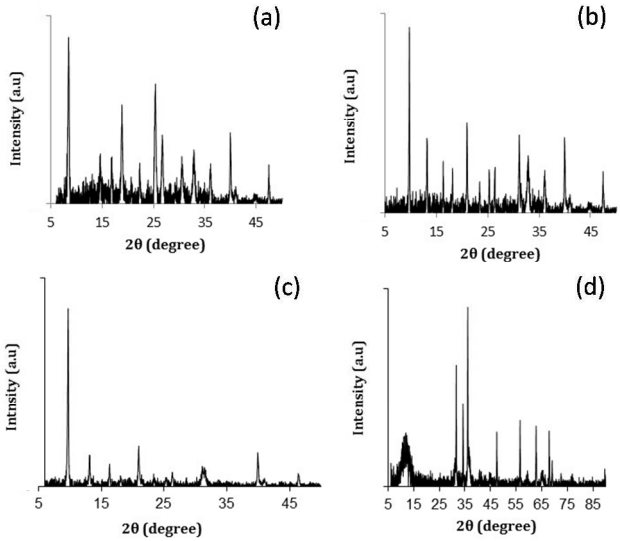

Figure 2. XRD patterns of a) Pt-RHO, b) Pt-DNL-6 and (c) Pt- SAPO-34 and d) Pt-hydrotalcite

Table. 1. Textural properties of the supports before and after Pt incorporation

Sample	**Surface area (m^2/g)**
RHO	**NA**
DNL-6	400
Pt-DNL-6 (salt1)	250
Pt-DNL-6 (salt2)	280
SAPO-34	490.4
Pt-SAPO-34 (salt1)	406.4
Pt-SAPO-34 (salt2)	478.2
Hydrotalcite	55
Pt-Hydrotalcite (salt1)	49
Pt-Hydrotalcite (salt2)	53

Figure 3 shows the decarboxylation of oleic acid over different catalysts as a function of temperature when salt

1(chloroplatinic acid) was used to incorporate Pt on the supports. As expected, over all these four catalysts (Pt-RHO, Pt-DNL-6, Pt-SAPO-34, Pt-Hydrotalcite) a higher degree of decarboxylation was observed at 325°C than at 245 °C. The same pattern was observed when these supports were impregnated with salt 2(tetrammine platinum nitrate) (Figure 4), The higher catalytic activity of Pt-based catalysts prepared from the $Pt(NH_3)_4[(NO_3)]_2$ has been reported earlier [5,17,37] Cationic complexes (like $Pt[(NH_3)_4]^{2+}$) probably lead to better dispersion / anchoring to the anionic O^{2-} centers on the catalyst surface ., and, consequently, of higher catalytic activity than anionic complexes of Pt (like $[PtCl_6]^{4-}$) . In the presence of H_2, oleic acid is first hydrogenated to stearic acid which then undergoes facile decarboxylation, In the absence of H_2, the hydrogenation route is not available and therefore thermal decarboxylation of the unsaturated acid is the only route available.

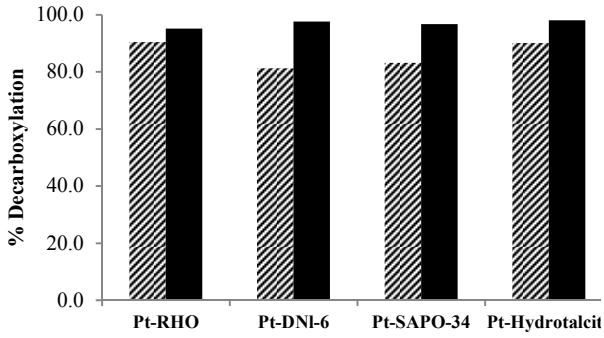

Figure 3. Decarboxylation of oleic acid over catalysts prepared by salt1at different reaction temperature (Reaction conditions: 40 ml oleic acid, 2 g catalyst, 2 hr, and pressure 20 bar at 245 and 325°C)

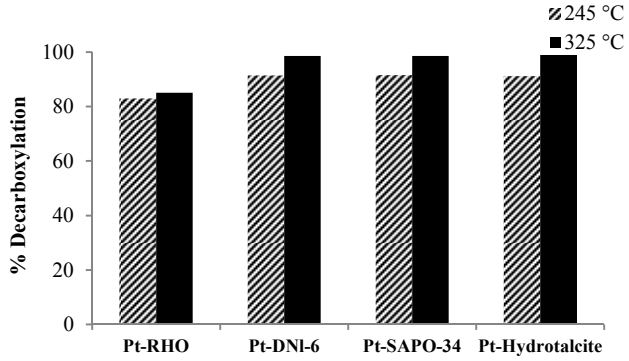

Figure 4. Decarboxylation of oleic acid over catalysts prepared by salt 2 at different reaction temperature (Reaction conditions: 40 ml oleic acid, 2 g catalyst, 2 hr, and pressure 20 bar at 245 and 325°C).

At 325 °C, when salt 1 was used as Pt precursor, the decarboxylation % was similar for all four catalysts (above 90%). However, when salt-2 was used , Pt-DNL-6, Pt-SAPO-34 and Pt-Hydrotalcite displayed high degree of decarboxylation (around 98%) . Decarboxylation in the presence of RHO was only ~ 85%.

Table 2. Acid numbers of decarboxylation product of oleic acid over catalysts prepared employing salt 1 and salt 2 at different reaction temperature (245 or 325°C)

Catalyst		Pt-RHO		Pt-DNL-6		Pt-SAPO-34		Pt-Hydrotalcite	
T (°C)		325	245	325	245	325	245	325	245
Acidity	Salt 1	9.7	19.3	4.9	37.6	6.6	33.9	4.0	19.8
	Salt 2	30.0	34.0	2.8	17	2.9	16.8	2.1	17.5

Table 2 shows the acid number of the reaction products (indicative of the concentration of unconverted fatty acid) over all these catalysts for the two salts employed to impregnate the supports. The acid number is lower at 325°C compared to 245°C for the all cases. According to the degree of decarboxylation and acid number it should be expected that the amount of carboxylic acid groups remaining in the product after the reaction should be lower at higher temperature.

Over all the catalysts except Pt-RHO, the acid number of the product (inversely proportional to the degree of decarboxylation) obtained using salt 2 as Pt precursor, is lower than that over the catalyst got using salt 1 as precursor. For Pt-RHO, decarboxylation over the catalyst using salt 1 was greater. The reasons are not clear. Differences in (a) the size of the Pt-RHO crystals (Figure 1) and (b) the Pt species present in aqueous solutions of salt 1 ([PtCl6]2- and salt 2 [Pt(NH3)4]2+ may, perhaps, shed more light on this point. The average size of the crystals in Pt-RHO is ~ 1.5 µm while the others are larger (2.3-3.0 µm). While the higher catalytic activity of Pt-based catalysts prepared from the Pt(NH3)4(NO3)2 is known [5,17,37], the greater activity of salt 1-derived catalysts in the case of Pt-RHO is surprising. In principle, the high concentration of exchangeable cations (Na, Cs) of zeolite RHO will lead to a high dispersion of the anionic ([PtCl6]2- complex rather than the cationic complex, [Pt(NH3)4]2+, derived from salt 2. This effect is reinforced in the smaller crystals of Pt-RHO leading to the high observed catalytic activity.

Stearic acid (and also other saturated carboxylic acid compounds) was formed by hydrogenation of oleic acid and then underwent decarboxylation to form heptadecane. The other components in the liquid product included branched paraffins formed by isomerization of the initially formed heptadecane, aromatics formed by cyclisation and aromatization (like dodecyl benzene) and lower molecular weight hydrocarbons (mostly C_6-C_{16} paraffins) formed by cracking of the heptadecane. No oleic acid was observed in the products under all reaction conditions, suggesting 100% conversion of oleic acid. The amount of stearic acid and other carboxylic acid groups in the product (such as nonanoic acid, decanoic acid and undecanoic acid) was lower at 325°C compared to 245°C for all catalysts which confirms that the highest degree of decarboxylation was observed at 325°C. Some alkenes such as undecene, dodecene, tridecene, tetradecene, hexadecene, heptadecene and octadecene were also observed in the products. The detailed product distribution is given in Table 3.

Catalyst	Product distribution (%wt)																						
	Salt	T (°C)	Hexane	Heptane	Octane	Nonane	Decane	Undecane	Dodecane	Tridecane	Tetradecane	Pentadecane	Hexadecane	Heptadecane	Octadecane	Nanodecane	UDB[1]	DDB[2]	Oleic acid	Stearic acid	Other Carboxylic[3] acid compounds	alkene[4]	%gas[5]
Pt-RHO	Salt 1	325	4.7	3.5	5.3	3.5	5.3	4.7	3	4.7	2.9	3.5	4.7	26.3	3.5	3	0	4.4	0	0.2	0.1	4.7	12
Pt-RHO	Salt 1	245	5.3	4.7	4.1	2.9	4.7	4.1	2.4	3.5	4.1	3.5	2.9	23.4	3.5	2.4	0	7	0	0.9	5.3	5.3	10
Pt-RHO	Salt 2	325	4	3.3	4.6	3.9	5	3.2	4.7	4	4.3	4.9	3.7	27	3.2	3.2	0	3.6	0	0.3	4	4.1	9
Pt-RHO	Salt 2	245	3.8	2.9	4.1	4.3	4.9	3.7	3.9	4.5	5.6	4.3	3.7	22	4.3	3.4	0.1	5.8	0	0.4	4.2	3.7	10.4
Pt-DNl-6	Salt 1	325	4.1	4.1	4.7	2.4	5.3	5.9	7.6	5.3	2.9	4.7	5.7	16.2	4.7	5.3	0	5.3	0	0.1	0	4.7	11
Pt-DNl-6	salt 1	245	5.3	4.1	3.5	6.3	4.1	5.3	5.9	3.5	4.7	2.3	5.1	10.8	4.1	4.1	0	5.3	0	7.6	4.1	2.9	11
Pt-DNl-6	Salt 2	325	4.1	2.9	4.1	4.2	2.9	2.5	3.5	3.3	2.4	2.9	2.4	47	2.4	1.8	0.5	2.9	0	0	0	0.2	10
Pt-DNl-6	Salt 2	245	4.8	4	5.5	4	3.4	2.8	3.4	4.5	5.7	4.9	3	30	3.6	3.9	0.1	3.3	0	0.4	2.3	0	10.4
Pt-SAPO-34	Salt 1	325	2.4	5.3	3.5	3.9	2.1	3.2	3.5	3.1	3.4	4.1	2.4	29.4	4.7	3.5	0	7.4	0	0.3	3.8	4	10
Pt-SAPO-34	Salt 1	245	2.7	5.1	3.8	2.7	4.7	3.9	3.5	3.9	4.6	4.3	3.4	23.5	4.7	3.6	0.2	7.8	0	0.5	4.2	2.9	10
Pt-SAPO-34	Salt 2	325	0.8	1.2	1.4	1.4	0.8	0.6	1.2	1.1	2.8	2.5	1.8	66.9	1	0.2	0	6	0	0.3	0	1	9
Pt-SAPO-34	Salt 2	245	2.6	1.5	2.3	2.2	3.4	2.2	2.4	2.7	2.1	3.9	3.2	50	1.2	0.9	0	6.2	0	0.7	1.1	0.9	10.5
Pt-Hydrotalcite	Salt 1	325	2.1	2.7	3.5	2.7	4.1	5.3	4.7	4.1	3.8	4.7	4.1	23.5	5.3	4.7	0.1	8.9	0	0.2	0	4.5	11
Pt-Hydrotalcite	Salt 1	245	2.1	3.7	3.8	2.7	5.4	5.3	4.7	4.1	4.5	4.7	4.1	20.6	5.3	4.7	0.1	7.9	0	0.5	0.1	4.7	11
Pt-Hydrotalcite	Salt 2	325	2.9	2.1	3.1	3.8	2.7	3.9	1.7	3.5	4.1	3.1	4.7	29.2	4.7	4.1	0	8.1	0	0	0	4.3	12
Pt-Hydrotalcite	Salt 2	245	1.8	2.4	3.5	4.1	2	2.8	4.1	4.6	4.7	3.5	4.1	27	4.7	3.5	0	7	0	0.6	3.5	4.1	12

[1] Undecylbenzene
[2] Dodecylbenzene
[3] Nonanoic acid, Decanoic acid, Undeanoic acid
[4] Undecene, Dodecene, Tridecene, Tetradecene, Hexadecene, Heptadecene, Octadecene
[5] Mass balance (CO_2,CH_4, others)

Figures 5 and 6 show the influence of reaction temperature and catalyst on selectivity to heptadecane, the linear C_{17} paraffin obtained by the decarboxylation of oleic acid when salt 1 and 2 were employed respectively. Heptadecane selectivity increased with temperature, and was favored in the presence of Pt-SAPO-34.

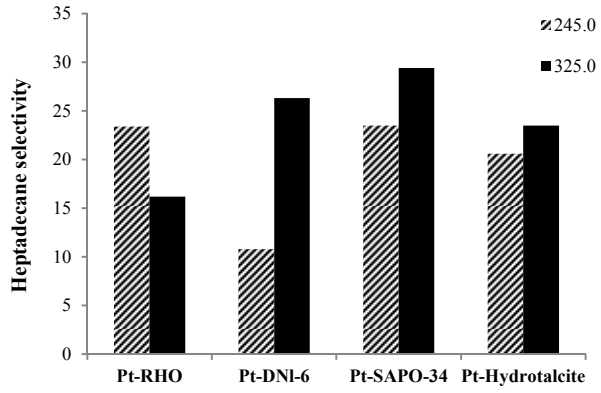

Figure 5. Effect of temperature and catalyst on heptadecane selectivity in the catalytic deoxygenation of oleic acid (Pt was impregnated on the supports from salt 1 , Reaction conditions: 40 ml oleic acid, 2 g catalyst, 2 hr and pressure 20 bar). Heptadecane selectivity (wt%)

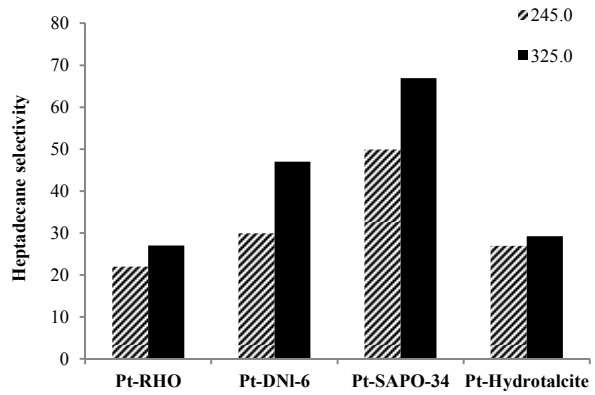

Figure 6. Effect of temperature and catalyst on heptadecane selectivity in the catalytic deoxygenation of oleic acid (Pt was impregrnated on the supports from salt 2, Reaction conditions: 40 ml oleic acid, 2 g catalyst, 2 hr and pressure 20 bar). Heptadecane selectivity (wt%)

Although Pt-DNL-6, Pt-SAPO-34 and Pt-Hydrotalcite displayed high degree of decarboxylation (around 98%) (Figure 1 and 2), selectivity to heptadecane was highest over Pt-SAPO-34. Pt-SAPO-34 has also the highest selectivity to dodecylbenzene (which is one of the most significant industrial products in this reaction) among other catalysts (Table 3). This can be partially explained by the difference in acidity of the supports. For example, RHO has lower strong acid sites and higher weak acid sites compared to SAPO-34. (RHO shows an NH_3 desorption peak at 170–200 °C which was assigned to weak acid sites, it' s second desorption peak is located at 480°C. the area of desorption peak for weak and strong acid sites were indicated to be around 150 and 75 respectively) [38, 39]. On supported metal, bifunctional catalysts, like those used in the present study, the selectivity for the initially formed linear paraffin, heptadecane (amongst the reaction products) is inversely proportional to the ability of the catalyst to isomerize it , further to branched paraffins over the acidic sites of the support. In addition to the acidity, the pore diameter of the support also plays a crucial role: Supports with smaller pore diameters prevent the further isomerization reaction of heptadecane since the large size of the transition state needed for the isomerization cannot be accomodated in the constrained confines of the small pores (restricted transition state selectivity [40]. In restricted transition state -type selectivity, certain reactions (like the isomerization of linear to branched olefins / paraffins are prevented because the transition state is too

large for the cavities of the catalyst. SAPO-34 belongs, structurally, to the chabazite group of zeolites. It contains 8-membered ring pores with openings of 0.38 nm. DNL-6 is structurally related to zeolite Rho with pore size of 0.36 nm (close to SAPO-34). Interestingly, both supports with very close pore size show the highest selectivity to heptadecane, suggesting "molecular sieving" effect. Zeolite Rho has also a pore system comprising of 8-membered rings. However, the pore openings can be as small as 0.29 nm. The other support hydrotalcite has a much larger pore diameter. The isomerization of heptadecane to bulkier branched isomers will, hence, be sterically more difficult, relatively, in the narrow pores of SAPO- 34 or DNL-6 than in the other two materials, accounting for its higher selectivity for the linear heptadecane. In the case of RHO, our results suggest that the smaller pore size may impose diffusion limitations.

Product selectivity profile in the presence of Pt-SAPO-34 is shown in Figures 7. Selectivity to heptadecane, increased with temperature and selectivity to other alkane products (C6-C16, C18 and C19) decreased with temperature (Figures 7). A heptadecane selectivity of 66.9% and dodecylbenzene selectivity of 8% were observed after 2hr in the presence of H_2 at 325 °C over Pt-SAPO-34.For all the catalysts employed in this study, higher degree of decarboxylation and selectivity to heptadecane were observed over the catalysts prepared with salt 2. The higher selectivity for heptadecane of the catalyst obtained using salt 2 (tetrammine platinum nitrate) might be related to the higher dispersion of Pt obtained when cationic complexes are used as precursors of Pt [5,17,36].

Table 1 also indicates that the heptadecane selectivity is influenced by the source of Pt; similar selectivity (~ 29%) is observed even for catalysts with different pore diameters when the Pt source is kept the same (salt 1) suggesting that the Pt source may be as important as the pore diameter in controlling the selectivity values. The presence of chlorine in salt 1 perhaps, modifies the nature of the pore system and, thereby, reduces the importance of the pore diameter in influencing product selectivity. Thus, (1) the acidity of the support, (2) the dispersion of the Pt and the (3) nature of the Pt source are all crucial factors in controlling the catalytic activity and product selectivity in the conversion of oleic acid to hydrocarbons.

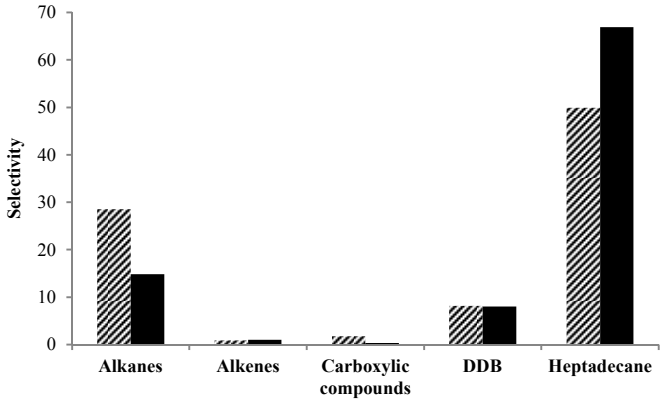

Figure 7. Effect of temperature on selectivity of the final products in the catalytic deoxygenation of oleic acid over Pt/SAPO-34. (Pt was impregrnated on the supports from salt 2, Reaction conditions: 40 ml oleic acid, 2 g catalyst, 2 hr, pressure 20 bar). Selectivity (wt%)

Figure 8 shows a representative TEM images of the Pt-SAPO-34 catalysts employed in this study. In particular, higher density of well-dispersed and smaller platinum nanoparticles on SAPO-34 support were observed when

salt 2 was used as Pt source (Figure 8b) as compared to salt 1 (Figure 8a) . In fact, Figure 8a shows the presence of Pt clusters, suggesting poor metal dispersion.

In general, for salt 2, the Pt particle histogram in Figure 9a, shows a higher fraction of small nanoparticles (in the 1-3 nm range) as compared to salt 1 (Figure 9b).

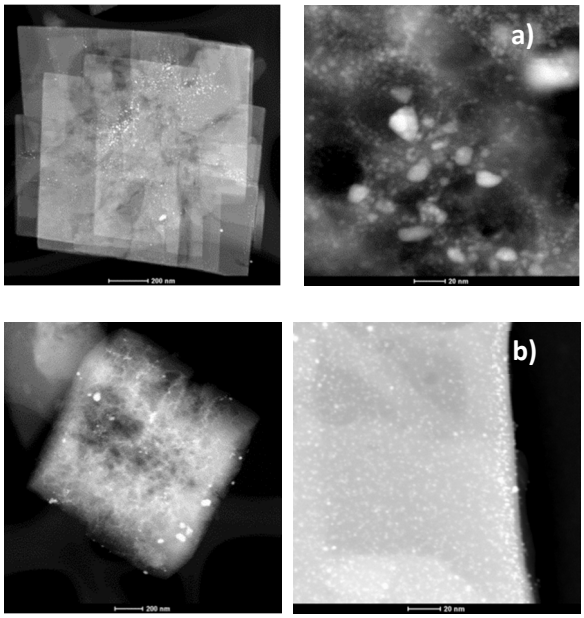

Figure 8. TEM images of 5 % Pt/SAPO-34 catalyst prepared from a) salt 1 (low and high magnification) b) using salt 2 (low and high magnification)

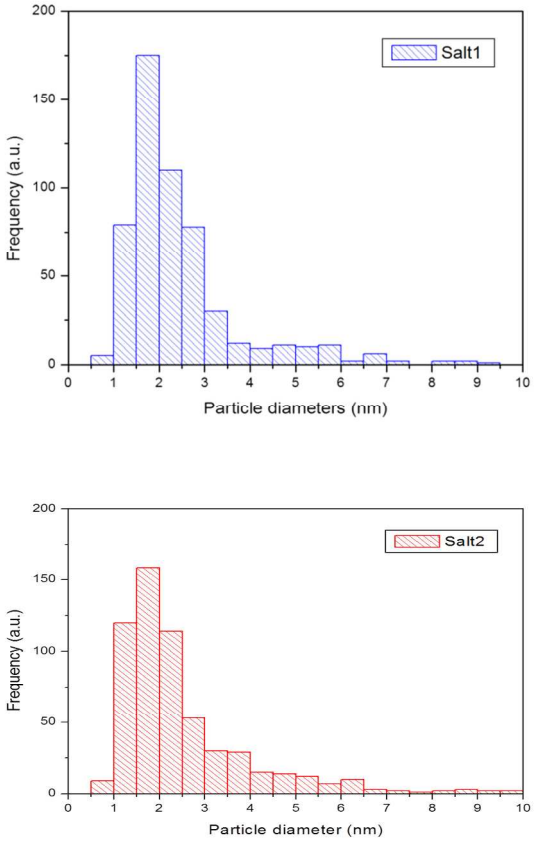

Figure 9. Pt particle size distribution histogram of 5 % Pt/SAPO-34 prepared using a) salt 1 and (b) salt 2

4. Conclusions

The decarboxylation and further conversion of oleic acid to gasoline /diesel-range hydrocarbons has been demonstrated over Pt/SAPO-34, Pt-DNL-6, Pt-RHO and Pt-hydrotalcite catalysts. The degree of decarboxylation and selectivity to the primary intermediate, the linear heptadecane are affected by reaction temperature and catalyst (support and nature of the Pt salt used for impregnation of the support). Higher temperatures increased the degree of decarboxylation (98%) and selectivity to heptadecane (up to ~66%). The initially formed paraffin intermediate undergoes further conversion to branched, cyclic and alkyl aromatic hydrocarbons. For example, dodecylbenzene, of

high interest in the petrochemical industry as a raw material for detergents, could be obtained in high yields. In the presence of acidic supports with narrow pore diameters, like SAPO-34, the degree of decarboxylation and selectivity to the linear paraffin, heptadecane, is high. The degree of dispersion of Pt within the porous support influenced the catalytic activity significantly. Higher degrees of decarboxylation and selectivity to heptadecane was observed over catalysts with more uniform and well dispersed Pt metal nanoparticles like those obtained when tetrammine platinum nitrate was used as the precursor of Pt. Catalyst acidity, the dispersion of Pt and the pore diameter of the support are the crucial factors determining the selectivity for the linear paraffin, heptadecane, in the product. Under more severe reaction conditions (higher temperatures) , significant quantities of hydrocarbons boiling in the gasoline range are formed by hydrocracking reactions over these catalysts**.**

Notes:

[a] Department of Chemical Engineering, University of Louisville, Louisville, KY, 40292.

[b] Conn Center for Renewable Energy Research, University of Louisville, Louisville, KY, 40292.

[c] Present address: 4, Lalit apts, Gulmohar Park, ITI road, Aundh, Pune-411007, India.

[d] Chemical and Biological Engineering Department, Colorado School of Mines, Golden CO 80401

* Corresponding author (mcarreon@mines.edu)

References

[1] I.Simakova, O. Simakova, P. Ma¨ki-Arvela, D. Murzin b. *Catalysis Today*, 2010**, 150***,* 28–31.

[2] J. Fu, X. Lu, P. Savage., *Chemistry & Sustainability, energy & materials (ChemSusChem),* 2011, **4**, 481-486.

[3] J. Fu, X. Lu, P. E. Savage, L. T. Thompson, Jr. Xiuyang Lu, *American Chemical Society Catalysis***.** 2011, **1**, 227–231.

[4] P. Arvela, B. Rozmysłowicz, S. Lestari, O Simakova, K. Eränen, T. Salmi, D.Yu. Murzin,. *Energy Fuels*, 2011, **25**, 2815–2825.

[5] E. Laurent, B. Delmon, *Appllied Catalysis A: General*. 1994, **109**, 77-96.

[6] M. Snåre, I. Kubickova, P.Arvela, K. Eranen, D. Yu. Murzin, *Industerial and Engineering Chemistry Research,* 2006, **45**, 5708-5715.

[7] M. Sna˚re, I. Kubickova, P. Maki-Arvela, D. Chichova, K. Eranen, D.Yu. Murzin, *Fuel*. 2008, **87**, 933–945.

[8] R. Stern, G. Hillion.; *US Pat*. 1985, **4**, 695,411.

[9] G.W. Huber, A. Corma, Angew. *Angewandte Chemie International Edition*. 2007, **46**, 7184–7201.

[10] S. Lestari, P. Maki-Arvela, K. Eranen, J. Beltramini, G.Q. Max Lu, D.Y. Murzin, *Catalysis Letter*. 2010, **134**, 250–257.

[11] H. Bernas, K. Eranen, I. Srimakova, A.R. Leino, K. Kordas, J. Myllyoja, P. Maki-Arvela, T. Salmi, D.Y. Murzin, *Fuel.* 2010, **89**, 2033–2039.

[12] M. Snåre, I. Kubickova, P.Arvela, K. Eranen, D. Yu. Murzin, *Catalysis Today*, 2005, **106** 197–200.

[13] M. Snåre, I. Kubickova, P.Arvela, K. Eranen, D. Yu. Murzin, *Catal Org React*, 2006, **115**, 415–25.

[14] D. Yu. Murzin, I. Kubickova, M. Snåre, P.Arvela, *European Patent Application*. 2005, 05075068.6.

[15] A. Sivasamy, K. Cheah, P. Fornasiero, F. Kemausuor, S. Zinoviev, S. Miertus, *Chemistry & Sustainability, energy & materials (ChemSusChem.),* 2009, **2**, 278 – 300.

[16] W. F. Maier, W. Roth, I. Thies and P. V. Ragué Schleyer, *Chemische Berichte*. 1982, **115**, 808-812.

[17] S. H. Bertram, *Chemisch. Weekblad*. 1936, **33**, 457-459.

[18] T. A. Foglia, P. A. Barr, *Journal of American Oil Chemist's Society*, 1976, **53**, 737-741.

[19] S. Lestari, P. Maki-Arvela, H. Bernas, O. Simakova, R. Sjonholm, J. Beltrami, G.Q.M. Lu, J. Myllyoja, I. Simakova, D.Y. Murzin, *Energy Fuels,* 2009, **23**, 3842–3845.

[20] F.A. Twaiq, N.A.M Zabidi, S.Bhatia, *Industerial and Engineering Chemistry Research,* 1999, **38**, 3230–7.

[21] WK. Craig, DW. Soveran, *US Pat*. 1991, 4,992,605.

[22] D. Lima, VC. Soares, EB. Ribeiro, DA. Caravalho, ECV. Cardoso, FC. Rassi, et al. *Journal of Analytical and Applied Pyrolysis*, 2004, **71,** 987–96.

[23] M. Arenda, T. Nonnena, W. F. Hoeldericha, J. Fischerb, J. Groosb, *Applied Catalysis A*: *General*. 2011, **399**, 198–204.

[24] T. Kasza, A. Holló, A. Thernesz, J. Hancsók , *Chemical Engineering Transactions*, 2010, **21**, 1225-1230.

[25] J. Hancso´k S. Kova´cs Gy. Po¨lczmann, T. Kasza, *Topics in catalysis*, 2011, **54**, 1094–1101.

[26] J.M. Campelo, F. Lafont, J.M. Marinas, *Applied Catalysis A: General*, 1998**, 170**, 139-144.

[27] P. Me´ riaudeau,1 V. A. Tuan, V. T. Nghiem, S. Y. Lai, L. N. Hung, and C. Naccache, *Journal of Catalysis*, 1997**, 169**, 55–66 .

[28] J. Walendziewski, B. Pniak, *Applied Catalysis A: General*, 2003, **250**, 39–47.

[29] Oleg V. Kikhtyanin, Anton E. Rubanov, Artem B. Ayupov, Gennadii V. Echevsky, Fuel 2010**, 89**, 3085–3092.

[30] M. Ahmadi, E. E. Macias, J.B. Jasinski, P. Ratnasamy, M.A. Carreon, *Journal of Molecular Catalysis A: Chemical ,* 2014, **386**, 14–19.

[31] Szostak, R. *Molecular Sieves:Principles of Synthesis and Identification*, Van Nostrand Reinhold, New York 1989**.**

[32]_X. Su, P. Tian, J. Li, Y. Zhang, S. Meng, Y. He, D. Fan, Z. Liu, *Microporous and Mesoporous Materials***,** 2011**, 144**, 113-119.

[33] T. Chatelain, J. patarin, R. Farre, O. Petigny, P. Schulz, *Zeolites*, 1996, **17**, 328.

[34] M. Palomino, A. Corma, J.L. Jorda, F. Rey, S. Valencia, *Chemical Communications,* 2012**, 48***,* 215.

[35] Frost, Ray and Martens, Wayde and Erickson, Kristy *Journal of Thermal Analysis and Calorimetry,* 2005**, 82**, 603-608

[36] Shiguang Li, Moises A. Carreon, Yanfeng Zhang, Hans H. Funke, Richard D. Noble, John L. Falconer, *Journal of Membrane Science* , 2010, **352** , 7–13

[37] A.T Madsen, E. Ahmed, C. H. Christensen, R. Fehrmann, A. Riisager, *Fuel*, 2011**, 90**, 3433–3438.

[38] Hee-Young Jeona, Chae-Ho Shina, Hye Ja Jungb, Suk Bong Hong, *Applied Catalysis A: General,* 2006**, 305**, 70–78

[39] Zeeshan Nawaz, Xiaoping Tang, Qiang Zhang, Dezheng Wang, Wei Fei, *Catalysis Comminucations*, 2009**, 10**, 1925–1930

[40] Sigmund M. Csicsery, *Pure & Applied Chemistry*, 1986**, 58(6)**, 841-856